



**HAL**  
open science

# A hybrid and adaptive segmentation method using color and texture information

C. Meurie, Y. Ruichek, A. Cohen, J. Marais

► **To cite this version:**

C. Meurie, Y. Ruichek, A. Cohen, J. Marais. A hybrid and adaptive segmentation method using color and texture information. IS&T/SPIE Electronic Imaging, Jan 2010, San Jose, United States. pp.75380R, 10.1117/12.838923 . hal-04757961

**HAL Id: hal-04757961**

**<https://hal.science/hal-04757961v1>**

Submitted on 29 Oct 2024

**HAL** is a multi-disciplinary open access archive for the deposit and dissemination of scientific research documents, whether they are published or not. The documents may come from teaching and research institutions in France or abroad, or from public or private research centers.

L'archive ouverte pluridisciplinaire **HAL**, est destinée au dépôt et à la diffusion de documents scientifiques de niveau recherche, publiés ou non, émanant des établissements d'enseignement et de recherche français ou étrangers, des laboratoires publics ou privés.

# A hybrid and adaptive segmentation method using color and texture information

Meurie C.<sup>1</sup> and Ruichek Y.<sup>1</sup> and Cohen A.<sup>1</sup> and Marais J.<sup>2</sup>

<sup>1</sup>Systems and Transportation Laboratory, University of Technology of Belfort-Montbéliard,  
13 rue Ernest Thierry Mieg, 90010 Belfort Cedex, France;

<sup>2</sup>Univ Lille Nord de France, Lille, France - INRETS, LEOST, Villeneuve d'Ascq, France,  
20 rue Elise Reclus, 59650 Villeneuve d'Ascq, France

## ABSTRACT

This paper presents a new image segmentation method based on the combination of texture and color informations. The method first computes the morphological color and texture gradients. The color gradient is analyzed taking into account the different color spaces. The texture gradient is computed using the luminance component of the HSL color space. The texture gradient procedure is achieved using a morphological filter and a granulometric and local energy analysis. To overcome the limitations of a linear/barycentric combination, the two morphological gradients are then mixed using a gradient component fusion strategy (to fuse the three components of the color gradient and the unique component of the texture gradient) and an adaptive technique to choose the weighting coefficients. The segmentation process is finally performed by applying the watershed technique using different type of germ images. The segmentation method is evaluated in different object classification applications using the k-means algorithm. The obtained results are compared with other known segmentation methods. The evaluation analysis shows that the proposed method gives better results, especially with hard image acquisition conditions.

**Keywords:** image segmentation, adaptive combination, color, texture, mathematical morphology

## 1. INTRODUCTION

Many segmentation methods are proposed in the literature. They can be grouped into two categories: edge and/or region based segmentation. These methods are usually developed considering specific applications. Therefore, there is no method that can be successfully applied for all applications. In the context of our applications, images present two important informations that are color and texture. It is hence useful to use a segmentation method based on these informations. ANGULO<sup>1</sup> proposes a segmentation method combining color and texture information. However, this method involves many parameters, which are difficult to adjust according to the considered application. This paper proposes to define a new segmentation method based on a non-parametric and adaptive combination of color and texture gradients. The proposed method uses an original technique to take into account both color and texture information by using an adaptive combination that considers local image content. This approach is tested on three databases. The first one is the Berkeley Segmentation Dataset and Benchmark (BSDB). The other databases concern two different applications: 1/ a transport application to identify the sky part of an image; 2/ a biomedical application to determine the global cells in the context of cancerous cells. In this paper, we focus on global cells extraction and mucus elimination (which is generally the major difficulty of the process since it causes bad statistics for suspicious cells detection).

The paper is organized as follows: Section 2 presents the morphological texture and color gradients definition. Section 3 describes the structural gradient process and the proposed strategy to combine texture and color gradients. In section 4, the color watershed based segmentation using the gradient combination is explained and illustrated on images of Berkeley Segmentation Database and Benchmark (BSDB). Before concluding, experimental results with real images are presented for different applications (transport and biomedical) in section 5.

## 2. MORPHOLOGICAL TEXTURE AND COLOR GRADIENTS DEFINITION

The process to obtain a texture gradient can be divided into the four following stages: 1/ Image filtering; 2/ Extraction of a texture layer; 3/ Granulometric analysis; 4/ Morphological texture gradient computation. The whole process of obtaining a texture gradient is based on mathematical morphology concepts and described in the literature (see<sup>1</sup> for details).

### 2.1 Image Filtering

The first stage of the process consists in image filtering. The aim is to simplify textures and delete structures/regions that are not significant for the final segmentation without losing the original objects outlines. The chosen filter is a connected leveling filter. This kind of filter preserves homogeneous zones and removes noise. Let  $f$  be an image,  $g$  a generic image called marker (usually defined as a simplification of the first image),  $\delta$  the morphological dilation and  $\epsilon$  the morphological erosion. The leveling operation can then be defined, for each pixel  $p$  of the image  $f$ , as the iteration until idem-potency of the following operations:

$$g' = \lambda(f, g) \quad (1)$$

$$g'_p = \begin{cases} f_p \wedge \delta(g)_p = \min(f_p, \delta(g)_p) & \text{if } g(p) < f(p) \\ f_p \wedge \epsilon(g)_p = \max(f_p, \epsilon(g)_p) & \text{if } g(p) > f(p) \end{cases} \quad (2)$$

The used marker is a simplification of the original image. It is obtained by means of an Alternating Sequential Filter (ASF), which is defined as a serie of morphological openings  $\gamma_n$  and closings  $\varphi_n$  of incremental size. The filtered image  $f'$  is obtained by the following relation:

$$f' = \lambda(ASF_n(f), f) \quad (3)$$

$$ASF_n(f) = \varphi_n \gamma_n \dots \varphi_2 \gamma_2 \varphi_1 \gamma_1(f) \quad (4)$$

### 2.2 Texture Layer

For the definition of a texture layer, only the luminance component of the HSL color space is taken into account, since texturing is a phenomenon associated to light intensity variation and not to wavelength (color). The texture layer, referred to as  $f_{tex}$ , is obtained as the difference between the luminance component of the original image  $f_l$  and the luminance component of the filtered image  $f'_l$  as  $f_{tex} = f_l - f'_l$ . Indeed, the filtered image can be interpreted as a non-textured image, while the original image contains textures as well as other information. By applying subtraction between these images, it is expected to remove all non-pertinent information and keep the textures.

### 2.3 Granulometric analysis

A granulometry is the study of the size distribution of the objects of an image based on the principle of sieving. It can be defined as a family of transformations  $(\Psi_n)_{n \geq 0}$  that depends only on a parameter  $n$  and has the following properties:

- $\Psi_0(f) = f$
- $\forall n \geq 0$ ,  $\Psi_n$  increasing:  $f \leq g \Rightarrow \Psi_n(f) \leq \Psi_n(g)$
- $\forall n \geq 0$ ,  $\Psi_n$  is anti-extensive:  $\Psi_n < Id$
- Absorption law:  $\forall n \geq 0, \forall m \geq 0, \Psi_n \Psi_m = \Psi_m \Psi_n = \Psi_{\max(n,m)}$

For a connected structuring element, the family of increasing openings  $(\gamma_n)_{n \geq 0}$  is a granulometry. The family of increasing closings  $(\varphi_n)_{n \geq 0}$  is considered as an anti-granulometry, or a granulometry for dark structures. Granulometric analysis of an image  $f$  consists in the evaluation of every opening of size  $n$  with a measure  $M$  defined as the addition of the values of the pixels of the opening:

$$M(\gamma_n(f)) = \sum_{p \in \gamma_n(f)} v(p) \quad (5)$$

Since an opening of size  $n$  is composed of all bright structures from  $f$  whose size is bigger than  $n$ ,  $M$  can be considered as the number of bright structures in  $f$  with a size bigger than  $n$ . By analogy, the same concept can be applied when  $M$  is computed for a closing. In this case, the measure refers to dark structures. At this stage, a Pattern Spectrum ( $PS$ ) can be defined as:

$$PS(f, n) = \begin{cases} M(\gamma_n(f)) - M(\gamma_{n+1}(f)) & \text{if } n \geq 0 \\ M(\varphi_n(f)) - M(\varphi_{n+1}(f)) & \text{if } n \leq -1 \end{cases} \quad (6)$$

$PS(f, n)$  measures the number of bright structures of size  $n$  in the image  $f$  if  $n > 0$  (resp. the dark structures if  $n < 0$ ). The pattern spectrum  $PS(f, n)$  (illustrated in figure 1) indicates the distribution of the structures associated to each scale  $n$ . It can be seen as a histogram. It can be used as a descriptor for texture classification. Nevertheless, it is computed globally for the entire image, while the expectation is to obtain more than one texture per image. Indeed, the classification should be applied for each pixel of the image  $f$ . To solve this problem, the granulometric analysis is computed locally for each pixel. This can be done by calculating  $PS(f_{W_x}, n)$  on a window centred on each pixel  $x$ . It is defined as the local energy image of size  $k$  that groups all the local pattern spectrum of size  $k$  of each pixel of the image. In a  $k$ -sized local energy image, the pixel associated to a structure of size  $k$  is affected with a high value. The images obtained by this procedure are then normalized.

## 2.4 Morphological texture gradient definition

A morphological texture gradient is defined using references to the concept of local energy image, presented previously. A morphological gradient is defined, for an image  $g$ , as the residue of dilatation and erosion (computed usually with a structuring element of size 1):

$$Q(g(x)) = \delta_\beta(g(x)) - \epsilon_\beta(g(x)) \quad (7)$$

The  $k$ -sized local energy image computed for the texture layer  $f_{tex}$  will be referred to as  $t_k$ . The texture gradient of the image is finally defined in reference to the morphological gradient of each  $t_k$ :

$$Q_{tex}(f_{tex}(x)) = \bigvee_{k \in K} [Q(t_k(x))] \quad (8)$$

where  $K$  is a set of numbers varying from  $[-n; n]$ .

## 2.5 Morphological color gradient definition

The classical definition of the morphological gradient for a gray scale image  $f$  is given by:  $\nabla f = \delta(f) - \epsilon(f)$ . The extension of gray scale image algorithms to color or vector valued images is not simple since there is no natural ordering on a set of color vectors, and more generally of multivariate data. According to Barnett,<sup>2</sup> there are several possible types of multidimensional vector orderings: marginal ordering, reduced ordering, partial ordering and conditional ordering. In this paper, the conditional ordering is considered.

Let  $x_1, x_2, \dots, x_n$  denote a set of  $n$   $p$ -dimensional vectors:  $x_i = \{x_{1(i)}, x_{2(i)}, \dots, x_{p(i)}\}, x_i \in R^p$ . In the conditional (also called lexicographic) ordering, the vectors are ordered according to a hierarchical order of their components. For two vectors  $x_i$  and  $x_j$ , one has:

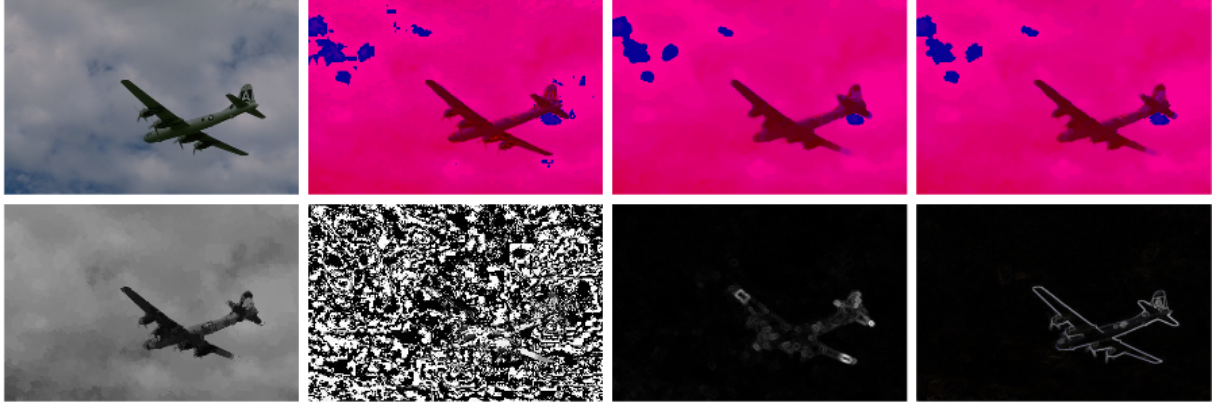


Figure 1. Illustration of calculation of gradients (top to bottom and left to right: original image, image in HSL color space, ASF, original Luminance; filtered Luminance; texture layer; texture gradient with  $K = \{-6, -4, -2, 2, 4, 6\}$ ), color gradient.

$$x_i \leq x_j \begin{cases} x_{1(i)} < x_{1(j)} \text{ OR} \\ x_{1(i)} = x_{1(j)} \text{ and } x_{2(i)} < x_{2(j)} \text{ OR } \dots \\ x_{1(i)} = x_{1(j)} \text{ and } x_{2(i)} = x_{2(j)} \dots x_{p(i)} < x_{p(j)} \end{cases}$$

If  $f$  is a color image,  $\delta(f)$  and  $\epsilon(f)$  are color vectors and the classical morphological color gradient  $f$  is given by:  $\nabla f = \delta(f) - \epsilon(f)$ . The morphological color gradient is illustrated in the figure 1.

### 3. STRUCTURAL GRADIENT DEFINITION

In order to achieve a robust and reliable segmentation, it is very useful to use both texture and color information. The main idea is to produce a structural gradient by combining the texture and color gradients. The problem is the fact that the color gradient is a color image while the texture gradient is a gray level image. To solve this problem, the proposed method starts by decomposing the color gradient image  $Q_{col}$  to obtain its three components which are  $Q_{col}^R$ ,  $Q_{col}^G$  and  $Q_{col}^B$ . In the next step, each component of the color gradient image is combined with the texture gradient image  $Q_{tex}$ . This operation produces three gray levels images  $Q^R$ ,  $Q^G$  and  $Q^B$ :

$$\begin{cases} Q^R = Q_{col}^R \otimes Q_{tex} \\ Q^G = Q_{col}^G \otimes Q_{tex} \\ Q^B = Q_{col}^B \otimes Q_{tex} \end{cases} \quad (9)$$

$Q^R$ ,  $Q^G$  and  $Q^B$  can be interpreted as the color components of a new color image, which is proposed to define the needed structural gradient. In other words, the structural gradient  $Q$  is defined as a color image with  $Q^R$  as the red component,  $Q^G$  as the green component, and  $Q^B$  as the blue component. This combination approach is suitable because, not only color information is preserved, but also the texture information is added to each color component. Indeed, texture, which is not a color phenomenon, is supposed to affect all colors equally. To combine a component of the color gradient image  $f$  and the texture gradient image  $g$ , three techniques are used: fixed combination, adaptive combination, supremum combination. An illustration of these combinations is given in figure 2. Let  $h$  be the output of the combination process which is applied for each pixel.

### 3.1 Fixed combination

The fixed combination is defined as a barycentric sum of the color gradient image and the texture gradient image. It uses a global weighting coefficient referred to as  $\alpha$ :

$$h(p) = \alpha f(p) + (1 - \alpha) \times g(p) \quad (10)$$

where  $\alpha$  is a constant coefficient taking its value in  $[0; 1]$ . The combination technique is not generally suitable, due to the coefficient  $\alpha$ , which is constant for the entire image. Indeed, one may need to give priority to color or texture according to their importance in the different zones of the image. This technique requires manual adjustment of the coefficient  $\alpha$  according to the content of the image.

### 3.2 Adaptive combination

The proposed adaptive combination strategy uses a modular combination of texture and color gradients according to the content of the image. It implies two advantages: First, it gives priority to the most important information (the color or the texture) for a given pixel. Second, it constitutes an automatic method, which can perform for all types of images. The adaptive combination is expressed as follows:

$$h(p) = \alpha_p f(p) + (1 - \alpha_p) \times g(p) \quad (11)$$

$\alpha_p$  is a coefficient taking its value in  $[0; 1]$ . It is calculated for each pixel  $p$  in order to give a high weight to the image that provides the most important information for the pixel. In other words,  $\alpha_p$  is high if the information is more important for  $f$  than for  $g$  (and vice-versa). It is computed as follows:

$$\alpha_p = \frac{f(p)}{f(p) + g(p)} \quad (12)$$

### 3.3 Supremum combination

Using the same principle as in the adaptive strategy, the supremum combination is sensibly different. There' is actually no combination at pixel level. Indeed, for a given pixel, the modular gradient is either a copy of the color gradient or the texture gradient depending on which one of them provides the biggest amount of information (the supremum). This combination has the same advantages as the adaptive one.

$$h(p) = \begin{cases} f(p), & \text{si } f(p) \geq g(p) \\ g(p), & \text{si } g(p) > f(p) \end{cases}$$

Figure 2 illustrates the different structural gradients according to the type of combination previously presented.

## 4. COLOR WATERSHED BASED SEGMENTATION

The watershed algorithm is one of the main mathematical morphology image processing operations.<sup>3,4</sup> It allows to segment an image into homogeneous regions from a seeds image (markers) and a potential image (gradient). Image segmentation based on the watershed algorithm has proved to be a powerful segmentation tool but, unfortunately, when directly applied to an image, this algorithm presents a strong over segmentation. One way to suppress this over segmentation is to use a non-parametric hierarchy of watershed, known as the waterfall algorithm.<sup>5</sup> Several authors propose different types of gradients including several orderings of color vectors.<sup>6-9</sup> But in the context of our transport application, the processing time of this approach would be too important. This is why we propose to define a specific image of seeds positioned experimentally and adapted to our applications. In the case of the other databases, the seeds correspond to a percentage of local minimum values (100% for the medical application, and 2% for the BSDb database). The watershed algorithm makes regions grow from the initial seeds using the priority given by the potential image (structural gradient based on color and texture information).



Figure 2. Illustration of different combination of gradients (top to bottom and left to right: original image, texture gradient, gradient with combination  $C=0.2/T=0.8$ , gradient with combination  $C=0.5/T=0.5$ , gradient with combination  $C=0.7/T=0.3$ , color gradient, gradient with adaptive combination, gradient with supremum combination).

## 5. EXPERIMENTAL RESULTS

In this section, we evaluate the proposed approach for image segmentation by combination of color and texture information using three databases. The tests concern the segmentation of eight images of the Berkeley Segmentation Dataset and Benchmark (BSD3). Others tests concern two different applications: 1/ a transport application to determine the percentage of sky in order to know the visibility of satellites; 2/ a biomedical application to determine the global cells. Cytoplasm and nucleus extraction, which allows statistical calculation for suspicious cells determination, is not explained in this paper. Instead, we will focus on global cells extraction and mucus elimination (which is generally the major difficulty of the process since it causes bad statistics for suspicious cells detection). To analyse the different segmentation and classification results, we use two evaluation methods (with reference segmentations/classifications): Global Coherence Error of the Martin's method (with reference segmentation), Good Classification Rate (with reference classification). For the BSD3 database and transport application, the influence of the color space is also studied for six color spaces ( $RGB$ ,  $HSL$ ,  $I_1I_2I_3$ ,  $YC_bC_r$ ,  $YCh_1Ch_2$ ,  $L^*a^*b^*$ ), each of them belonging to one of the six main color space families described in the literature.<sup>10</sup> Considering a PC Centrino II (2.8 Ghz, 4Go RAM), the processing time of the proposed method is 83s. This time is relatively high and corresponds to the calculation of the texture gradient. The rest of the treatment is inferior to 1s. We actually work on the calculation of the texture gradient in real time.

Figure 3 illustrates segmented images for different gradient combinations on the Berkeley Segmentation Database and Benchmark (BSD3). We can notice that the segmentation obtained with a combination of 20% color and 80% texture gives very bad results. The plane, the branch, the woman's face and the surfer are not correctly segmented. The results obtained with a combination of 50% color and 50% texture are better except for the buffalo, the man arm and the surfer. A combination of 70% color and 30% texture seems to give the best results for the fixed combination. However, the rudder of the plane is not well extracted and the surfer is roughly segmented. To conclude, the best weighting coefficient for the fixed combination depends on the content of the image (for example: 50% color and 50% texture for the plane and 70% color and 30% texture for the surfer). On the other hand, even if the adaptive combination is better than the supremum combination, the both methods give very good results (except for the rocks image) and have the major advantage of being non-parametric. Figure 6 (left) shows the influence of color spaces for the segmented images of the BSD3 database. We must point out that in order to use the fixed combination, the best color space must be chosen depending of the weighting coefficients. For the  $RGB$  color space, the best combinations are the adaptive and supremum. If we consider all the combinations and the six color spaces, the best results are those obtained by the adaptive combination for the  $RGB$  color space.

The first tested application concerns positioning systems for Intelligent Transportation Systems. Most of



Figure 3. Segmented images with different gradient combinations in Berkeley Segmentation Database and Benchmark (top to bottom : initial image, segmented images (with  $C=0,2/T=0,8$ ; with  $C=0,5/T=0,5$ ; with  $C=0,7/T=0,3$ ; with adaptive combination, with supremum combination)).

positioning systems are based on GNSS (Global Navigation Satellite System) such as GPS. As other radio-navigation solutions, satellite-based systems use propagation time measurements for positioning. Indeed, each satellite of the constellation broadcasts continuously its own signal and the role of the receiver is to estimate the propagation time in order to translate it into a distance, called pseudorange. By triangulation, three simultaneous pseudoranges allow the receiver to compute its position in a 3D absolute referential. However, in constrained environments such as urban area, signals can be reflected or blocked by obstacles (building, trees, ...). Reflections add a delay to the propagation time estimation, especially when the direct path of the signal is not available. In order to ensure a safe and accurate position to the user, mitigation or derived techniques can be used.<sup>11-16</sup> A system using a video record of the environment surrounding the GPS antenna has been developed for the first version of the PREDISSAT tool.<sup>14</sup> The goal of the technique proposed in this section is to benefit from new advances in image processing to enhance satellite state reception determination by a better detection of masking elements. For that, the process starts by segmenting the image into regions of interest according to a given criteria (color and texture). The obtained regions have to be classified into at least two classes: the sky and the rest of the image (vegetation, buildings, ...).

In terms of segmentation (cf. figure 4), the results obtained when taking into account the color information only are quite satisfying for urban images. This is not surprising since color information is more important for this kind of images than texture information. For other kinds of images (cloud and vegetation), sky regions are usually over-segmented and the sunny zones are mostly dilated when using only color information. This problem is also present (though in a smaller amount) with a combination of 80% color and 20% texture. On the other hand, the segmentation results computed using mostly texture information (combination of 20% color and 80% texture) are never satisfying enough. The best segmentation results are those computed using a fixed combination of 50% color and 50% texture or the adaptive method presented in this paper (lines fifth and sixth of figure 4). The results are, indeed, very satisfying. Nevertheless, some inconsistencies are still present on certain images segmented using the fixed combination. For example, in the second image, a small region appears on the bottom because of the excessive amount of sun. Another example is the seventh image in which the sky is divided into two regions instead of one. As for the sixth image, results obtained with a combination of 80% color and 20% texture beat those obtained with a combination of 50% color and 50% texture. This clearly demonstrates that



the best parameters for the fixed method vary from image to image. These inconsistencies are not present when applying the supremum or adaptive methods, which don't require any parameters adjustment. The supremum and adaptive methods work very well for all kinds of images, specially those featuring great amounts of sky and vegetation. As for classification, the last row of figure 4 and figure 6 (middle) illustrate the results according to the best (figure 4) and all (figure 6 (middle)) combination techniques. The last row of the figure 4 illustrates the classification results (according to the classification of reference) into two classes (sky and not-sky regions) obtained with the k-means algorithm for the best combination. The proposed approach based on an adaptive strategy performs very well for all image types. If we consider the *RGB* color space and the average percentage of well classified pixels over all images, the adaptive method takes the first place with an average of 95.3%. The 50% color and 50% texture fixed combination takes the second place with an average of 94,6%. With the proposed adaptive combination technique, the classification rates are globally equivalent, compared with those provided by the fixed combination. The major advantage of the adaptive method is that it allows automatically to take into account the local content of the image and it requires no parameters settings. Figure 6 (middle) illustrates the influence of the color spaces on classification rate. The fixed combination of 50% color and 50% texture gets the best results in  $YC_bC_r$  color space.  $L^*a^*b^*$  is the best color space if only color information is taken into account. To conclude, it may be useful to choose the color space that is the most suitable when using the fixed combination. This can be seen as a new parameter for the fixed combination method. On the contrary, the proposed adaptive method gives the best results in *RGB* color space and therefore requires no studies on the choice of a color space.

The second application concerns biomedical and, more particularly, the detection of suspicious cells in bronchial cytology. In the context of this work, the extraction of the different cellular objects (cytoplasm and nucleus) for statistical calculation in order to determine the presence of suspicious cells won't be presented. Our main is global cells extraction and mucus elimination (which actually represents the major difficulty as it results in inaccurate statistics). Previous works based on the segmentation of microscopic color images (using only the color information) give satisfactory results,<sup>7,17</sup> but it requires a combination of decisions provided by several classifiers. In this paper, we demonstrate that the new segmentation approach using color and texture combination can be applied to the biomedical application and can give very good results. Moreover, these results are even better than those provided by the previous works for certain cases. The process starts by segmenting the image into regions of interest according to a given texture/color criteria. The obtained regions are then classified into two classes (the global cell and the background) with the k-means algorithm.

Figure 5 illustrates original microscopic images of bronchial cytology and their classification results using k-means with the different combinations (C=0,2/T=0,8; C=0,5/T=0,5; C=0,7/T=0,3; adaptive combination, supremum combination). Previous works<sup>7,17</sup> show that it is very difficult to extract the mucus without a specific strategy and a combination of classifiers. Nevertheless, it would be interesting to merge previous works with the proposed approach in order to increase the robustness of our algorithm. If we consider the results illustrated in figures 5 and 6 (right), we can see that the proposed method gives the best results. The biggest improvement can be seen on the first image of figure 5 where the mucus is completely eliminated when using the adaptive combination (line 6). This is not the case for the fixed combination method (lines 3 to 5). For this application, if we consider a fixed combination, a weighting coefficient of 100% color gives in average, the best results. This coefficient is different from the one found for the transport application. This means that parameters must be redefined when using the fixed combination method. This constraint is not considered when using the proposed non-parametric combination method. To conclude, a good classification rate of 96,5% is obtained for the proposed method while the fixed combination provides results with a rate classification inferior to 77,2% is obtained.

## 6. CONCLUSION

A new segmentation technique that combines both color and texture information is proposed. The originality of the method is that it takes into account local image content by automatically computing the weighting coefficients for color and texture. The classical technique uses a fixed combination and requires the choice of the best color space and a manual adjustment of the weighting coefficients, which are global for all the pixels of the image. On the contrary, the proposed method does not require any parameters settings. The adaptive method is evaluated for three databases (Berkeley Segmentation Dataset and Benchmark, transport and biomedical applications) and

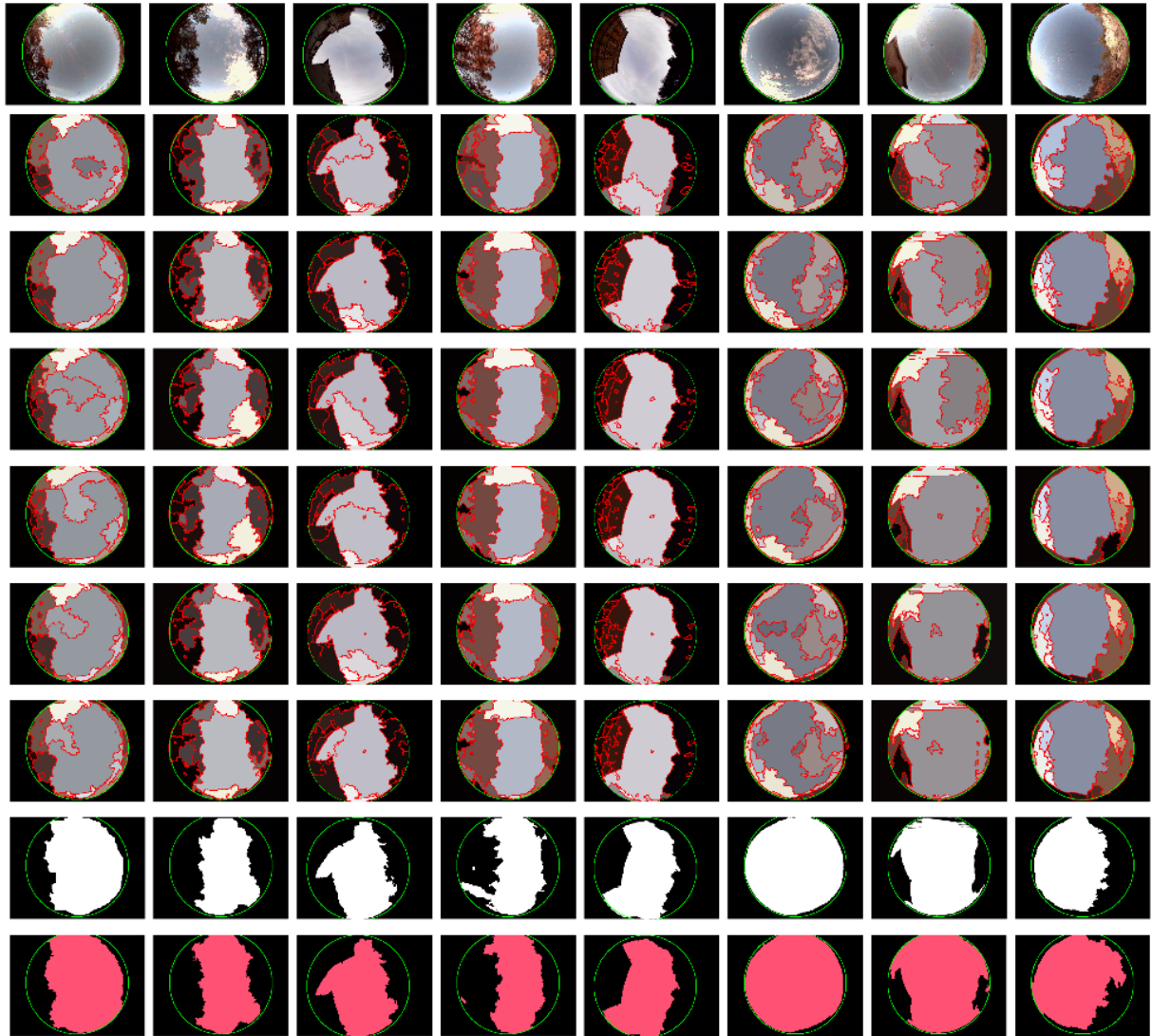


Figure 4. Segmented and classified images with k-means and different gradient combinations for transport application (top to bottom : initial image, segmented images (with  $C=0,2/T=0,8$ ; with  $C=0,5/T=0,5$ ; with  $C=0,8/T=0,2$ ; with  $C=1/T=0$ ; with adaptive combination, with supremum combination), reference classified image, classified images with the best combination).

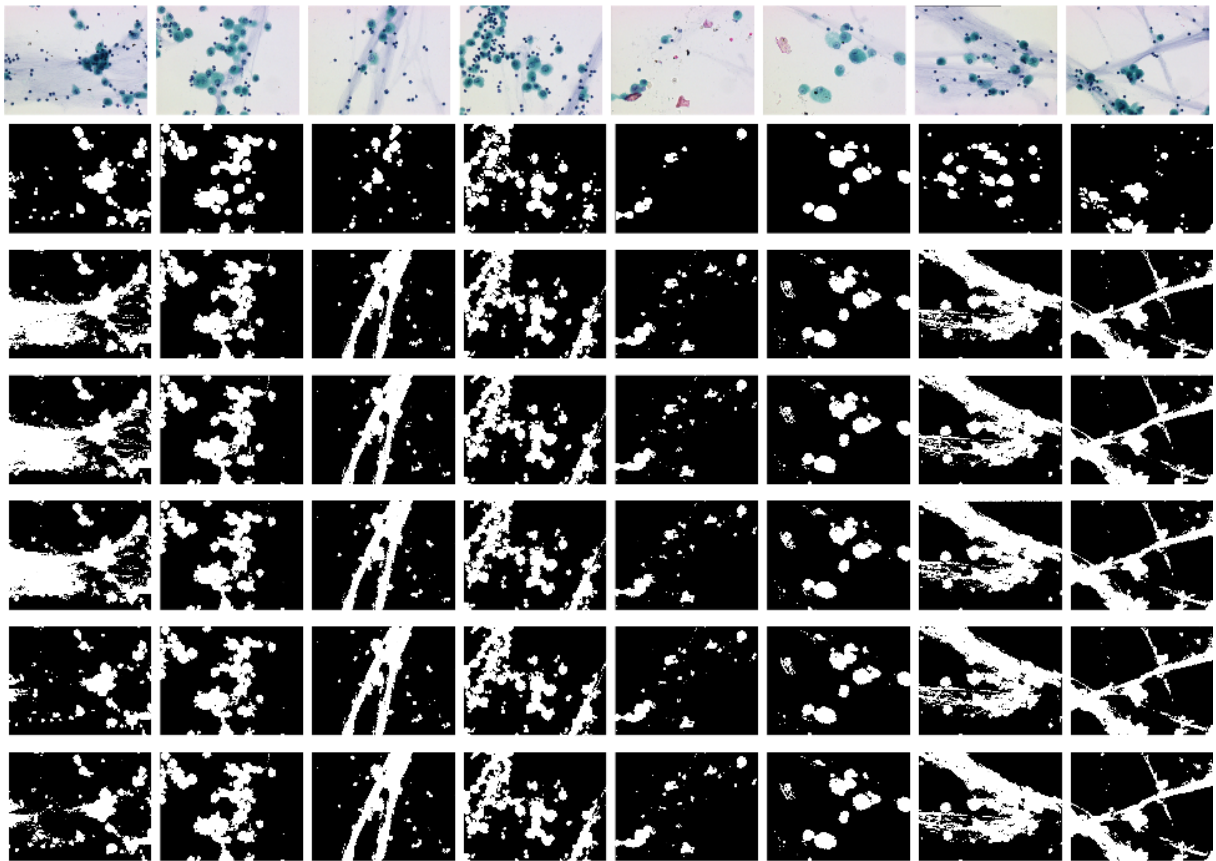


Figure 5. Classified images with k-means and different gradients combinations for biomedical application (top to bottom : initial image, reference classified image, classified images with k-means and with  $C=0,2/T=0,8$ ; with  $C=0,5/T=0,5$ ; with  $C=0,7/T=0,3$ ; with adaptive combination, with supremum combination).

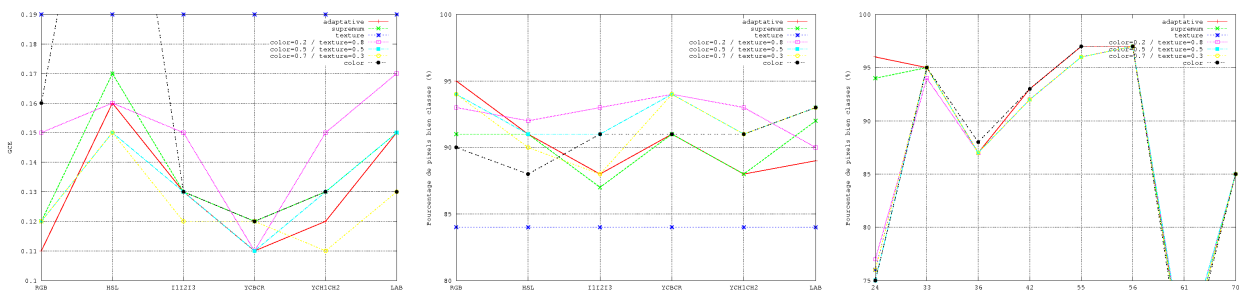


Figure 6. Evaluation of segmented/classified images in different color space and for several databases (left to right : BSD3 (with GCE), transport application (with Good classification rate), and biomedical applications (with the good classification rate))

provides very good results. On the first part, the technique is used for characterizing the environment of GNSS signals reception and more particularly for estimating the percentage of visible sky (95,3% VS 94,6%). On the second part, the method is used for global cells extraction on microscopic images and provides the best results (90% VS 87,5%). The classification results for the proposed method are very satisfactory considering those obtained by the other methods which present a parameter adjustment difficulty. Future works are in progress and concern the analysis in terms of different color and texture gradients and the calculation of the texture gradient in real time.

## ACKNOWLEDGMENTS

The research works presented is a part of the ViLoc project, supported by the Regional Council of Franche-Comté (France).

## REFERENCES

- [1] Angulo, J., “Gradients morphologiques de texture. application à la segmentation couleur+texture par lpe,” in [*COmpression et REprésentation des Siganux Audiovisuels*], 42–47 (Nov. 2006).
- [2] Barnett, V., “The ordering of multivariate data,” *Journal of the royal society of statistics* **A139**(3), 318–355 (1976).
- [3] Vincent, L. and Soille, P., “Watersheds in digital spaces : an efficient algorithm based on immersions simulations,” *IEEE Trans. On Pattern Analysis and Machine Intelligence (PAMI)* **13**(16), 583–598 (1991).
- [4] Shafarenko, L., Petrou, M., and Kittler, J., “Automatic watershed segmentation of randomly textured color images,” *IEEE Trans. On Image Processing* **6**(11), 1530–1543 (1997).
- [5] Beucher, S., “Watershed, hierarchical segmentation and waterfall algorithm,” *Mathematical morphology and its applications to image ans signal processing* , 69–76 (1994).
- [6] Angulo, J. and Serra, J., “Color segmentation by ordered mergings,” in [*International Conference on Image Processing (ICIP)*], **2**, 125–128 (2003).
- [7] Meurie, C., *Segmentation of color images by pixels classification and hierarchy of partitions*, PhD thesis, University of Caen Basse-Normandie, Caen, France (Oct. 2005).
- [8] Lezoray, O., Meurie, C., and Elmoataz, A., “A graph approach to color mathematical morphology,” in [*IEEE Symposium on Signal Processing and Information Technology (ISSPIT)*], 856–861 (2005).
- [9] Lezoray, O., Meurie, C., and Elmoataz, A., “Graph-based ordering scheme for color image filtering,” *International Journal of Image and Graphics* **8**, 473–493 (July 2008).
- [10] Vandenbroucke, N., *Segmentation d’images par classification de pixels dans des espaces d’attributs colorimétriques adaptés*, PhD thesis, University of Lille 1 (Dec. 2000).
- [11] Lentmaier, M., Krach, B., and Robertson, P., “Bayesian time delay estimation of gnss signals in dynamic multipath environment,” *International Journal of Navigation and Observation (ID 372651)*, 11 (2008).
- [12] Wang, J.-H. and Gao, Y., “High-sensitivity gps data classification based on signal degradation conditions,” *IEEE Trans. On Vehicular Technology* **56**, 566–574 (Mar. 2007).
- [13] Viandier, N., Nahimana, F., Marais, J., and Duflos, E., “Gnss performance enhancement in urban environment based on pseudo-range error model,” in [*IEEE/ION Position Location And Navigation System (PLANS)*], 6 (May 2008).
- [14] Marais, J., Berbineau, M., and Heddebaut, M., “Land mobile gnss, availability and multipath evaluation tool,” *IEEE Trans. On Vehicular Technology* **54**, 1697–1704 (Sept. 2005).
- [15] Meguro, J., Murata, T., Takiguchi, J.-I., Amano, Y., and Hashizume, T., “Gps accuracy improvement by satellite selection using omnidirectional infrared camera,” in [*EEE/RSJ International Conference on Intelligent Robots and Systems*], 22–26 (Sept. 2008).
- [16] Meguro, J.-I., Murata, T., Takiguchi, J.-I., Amano, Y., and Hashizume, T., “Gps multipath mitigation for urban area using omnidirectional infrared camera,” *IEEE Trans. On Intelligent Transportation Systems* **10**, 22–30 (Mar. 2009).
- [17] Meurie, C., Lezoray, O., Charrier, C., and Elmoataz, A., “Combination of multiple pixel classifiers for microscopic image segmentation,” *IJRA (IASTED International Journal of Robotics and Automation)* **20**(2), 63–69 (2005). Special issue on Colour Image Processing and Analysis for Machine Vision, ISSN 0826-8185.